Journal of Nuclear Materials 85 & 86 (1979) 817–822

DEVELOPMENT OF MECHANICAL PROPERTY CORRELATION METHODOLOGY FOR FUSION ENVIRONMENTS*

G. R. ODETTE and D. FREY

University of California, Santa Barbara
California, 93016 USA

It is suggested that a model-based analysis of the relationship between microstructure and properties and relatively simple properties, such as tensile data, and fracture/failure parameters is one useful component in the overall effort to predict structural response in fusion reactor environments. The approach is applied to modeling yield strength changes in irradiated stainless steel with apparent success. Further analysis of ductility data may suggest significant changes in fracture mechanisms in highly irradiated stainless steel. Finally, a simple micromechanical model is used to estimate changes in fracture toughness; while there is not sufficient confirmatory data, the calculations indicate a substantial reduction in toughness due to irradiation.

1. INTRODUCTION

In-service mechanical property degradation leading to premature failures of fusion first wall structures is potentially one of the most serious obstacles to commercial fusion power.

Alloy development and fusion design efforts are confronted by at least three major problems when attempting to assess the effect of in-service irradiation, including:

1. There is no completely proper materials test environment in terms of appropriate combinations of neutron spectrum, flux, volume, and time history of temperature, flux (ϕ) and stress, which simulates the fusion environment.
2. The most proper high flux test environments will have small irradiation volumes (<1000 cm^3 for $\phi > 10^{14}$ n/cm^2-sec and < 10 cm^3 for $\phi > 10^{15}$ n/cm^2-sec).
3. There are a large number of potential structural failure modes ranging from creep rupture to catastrophic fracture.

In order to relate the data obtained in test irradiation environments to conditions in fusion reactors, a proper correlation methodology which rests on a firm physical understanding of the radiation effects and on structural failure modes is needed. One important component of such a methodology is developing a better understanding of the relationship between microstructure and properties and simple properties and fracture parameters (other components include: high energy neutron and fission reactor data base development; extracting useful mechanical property information from very small test volumes; and establishing the connection between properties/fracture parameters and design criteria). Understanding the relationship between microstructure and properties would not only be beneficial in optimizing the use of the small test volume in high energy neutron facilities, and in providing a better basis for extrapolating fission reactor data, but also might promote more rapid advances in the development of irradiation resistant alloys. At least three general classes of analytical tools can be used in such studies, including: micromechanical models of flow and fracture; flow, fracture and corresponding microstructure maps; and advanced test/failure analysis methods, including finite element techniques.

Preliminary results of correlating microstructure and yield stress in irradiated 316 stainless steel are presented. An empirical relationship is used to relate yield and ultimate stess to uniform elongation. Extension of this general approach to other fracture modes is also discussed briefly, with specific application to plane strain fracture toughness.

2. CORRELATING THE YIELD STRESS OF STAINLESS STEEL WITH IRRADIATION MICROSTRUCTURE

Because of the extensive data on both microstructure and properties, 316 austenitic stainless steels were used as a starting point in the attempt to correlate irradiation microstructure to yield stress changes. While there have been some limited attempts at establishing such correlations [1-3], no systematic attempt to link the overall microstructure and property data bases has been made previously.

Four distinct microstructural features were treated in the correlation model developed in this work including gas bubbles, voids, dislocation loops, and network dislocations. Solute redistribution or phase instabilities due to irradiation were not treated. However, because of the strong intercorrelations with the development of other microstructural features, such microchemical variations may be implicitly included as covariances in the current correlations. Ultimately, when sufficient data is available, microchemical features should be directly included in the models; indeed, this may be crucial to extending the approach to properties such as creep rupture.

The evolution of the microstructural features

*This research was sponsored in part by the DOE Office of Fusion Energy, Contract No. EY-76-5-0034.

was modeled as follows: for bubbles (b), voids (v), and loops (ℓ) a radius-density parameter $rN_{b,v,\ell}$ was defined in parametric forms $f_{b,v,\ell}(T,dpa)$ approximating data trend curves and/or model based predictions of microstructural development [4]. Similarly, the total network dislocation density $\rho_n = f_n(T,dpa)$ was determined from the data base or equivalent model predictions [4]. Some illustrative plots of these parametric functions are shown in Fig. 1.

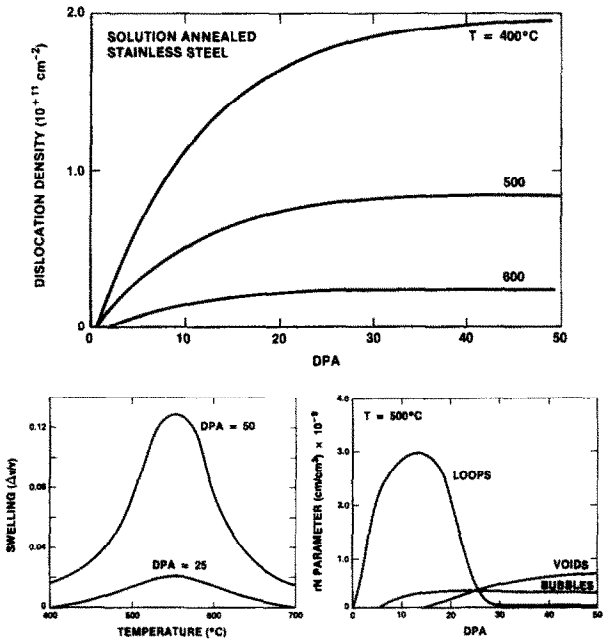

FIGURE 1. Illustration of Parametric Microstructure Models Used in the Correlation.

These parametric microstructure models were then combined with simple dislocation hardening theories to predict yield stress changes as

$$\sigma_{ys} = 2\sqrt{\left[\sum \frac{Gb\sqrt{2Nr_i}}{\beta_i}\right]^2} + K\sqrt{\rho_n} + \sigma^o_{ys} \qquad (1)$$

where G is the shear modulus, b the Burgers vector, β_i strength parameter for obstacle i, K an empirical network dislocation ρ_n strength constant and σ^o_{ys} the initial yield stress. Based on theoretical considerations, linear superposition was used to aggregate the contributions from the combined cavities and loops, the network dislocations and the initial yield stress [5]. A square root superposition summation was used to find the total contribution of short-range obstacles (cavities and loops) [5]. The empirical value of K was estimated by using strength differences between solution annealed and cold worked-steel in the unirradiated condition (Note, $K \sim Gb/2\pi$) as

$$K(T_o) = \frac{\left[\sigma^o_{ys}(cw, T_o) - \sigma^o_{ys}(SA, T_o)\right]}{\left(\sqrt{\rho_n^{cw}(T_o)} - \sqrt{\rho_n^{SA}(T_o)}\right)} \qquad (2)$$

below appreciable recovery temperatures ($T_o < 500°C$). A small correction for modulus change with temperature was used to derive a temperature dependent $K(T) = K(T_o)\,G(T)/G(T_o)$. Dislocation density recovery in the cold-worked condition was approximately accounted for using experimental values at the unirradiated yield stress -- i.e. $\rho_o^{cw}(T) \propto [\sigma^o_{ys}(cw.T)]^2$.

The strength parameters β_i can be estimated from any one of a number of dislocation obstacle hardening theories [5]. Because of significant uncertainties in the microstructure data approximate values are sufficient for purposes of this analysis. Hence, a moderate to strong barrier model was assumed for both cavities and loops, leading to a common $\sqrt{Nr}$ incremental strengthening dependence. Voids were taken as strong Orwan barriers $\beta_v \sim 1$, and loops and bubbles as medium strength barriers, with $\beta_\ell \sim 3$ and $\beta_b \sim 5$ (assuming the bubble radius is ~ 5 times the dislocation core radius) [5].

Figure 2a and 2b show some typical model pre-

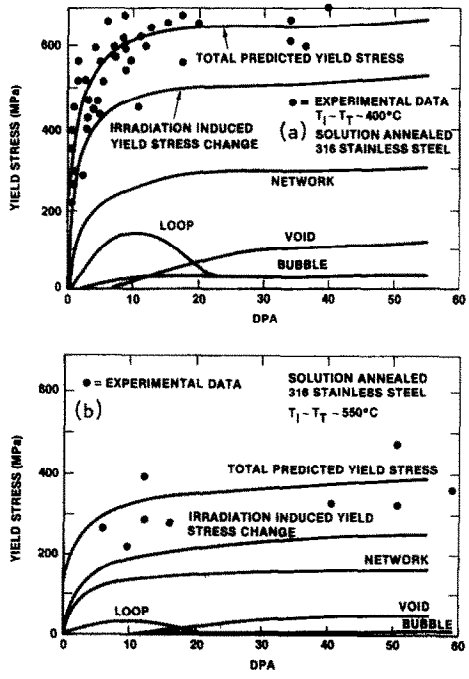

Figure 2. Comparisons of Model Predictions with Data for 316 Solution Annealed Stainless Steel at a) 400°C and b) 550°C.

dictions of yield stress changes as a function of exposure compared to a set of data [6] for solution annealed 316 stainless steel at $T_i \sim T_T \sim 400°C$ and 550°C respectively. Roughly equivalent results were found for data-model comparisons over the range of T ~400° - 700°C. Figure 3 shows a plot for cold-worked 316 stainless steel [7], and Figure 4 an overall comparison of model predictions versus measured yield strength data.

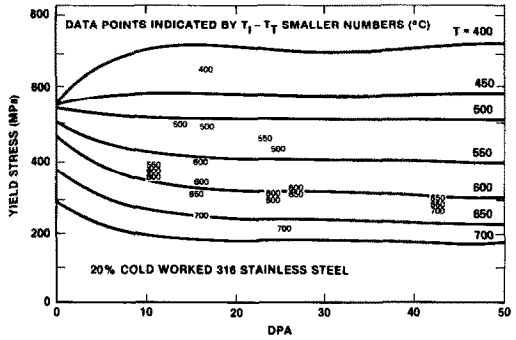

Figure 3. Comparisons of Model Predictions with Data for 20% Cold-Worked 316 Stainless Steel at Various Temperatures.

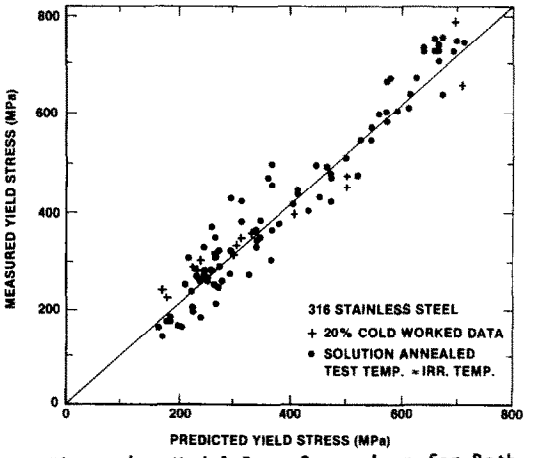

Figure 4. Model-Data Comparison for Both Cold-Worked and Solution Annealed Stainless Steel.

Clearly, both the qualitative trends and the quantitative values of the data are predicted by the model. While the quantitative agreement is satisfying, the qualitative consistency is probably most significant, in view of various approximations in the model. Returning to Figures 2 and 3 it is evident that: 1) the major increases in yield strength are due to an increase in network dislocation density; 2) the rapid rise in yield stress in the exposure regime below where void swelling is significant is due to the increases in network and loop dislocation densities; and 3) the saturation in yield stress increases is associated with a saturation in the dislocation microstructure and cavity densities, with additional increases occurring only with void growth at a low rate, $(\text{swelling})^{1/6}$. The decrease in yield stress in irradiated cold worked materials is due to additional irradiation and/or thermal recovery. It should be noted, that in this particular set of calculations the decrease in the loop density parameter $(Nr)_\ell$ at high fluences may be exaggerated, particularly at low temperatures. This is not terribly significant to the results, however, since the hardening of a net dislocation line length in loops is approximately equivalent to the hardening due to an equivalent line length of network dislocation. Hence, a higher assumed network density would partly compensate for a lower assumed loop density. Indeed, some of the larger loops may unfault at low strains and, therefore, behave much like line dislocations.

Agreement is not as good if the data base for comparison is extended, probably indicating a wider range of microstructural variations. This is shown in Figure 5 when the predicted saturation yield is plotted against temperature and compared to several sets of data [1, 6, 8, 9]; it is notable, however, that in spite of increased scatter, the proper trend is maintained. Indeed, one of the practical uses of such models is to carry out sensitivity studies by varying model parameters over appropriate ranges in order to estimate the contributions of various sources of data scatter. Preliminary sensitivity studies indicate that yield stress scatter is consistent with observed variations in the microstructural features treated in the model. Finally, it is important to emphasize that the microstructure model may not precisely reflect the detailed mechanisms, in particular as influenced by concommitant changes in microchemistry. However, the ability to correlate microstructure with an important mechanical property over a wide range of conditions is clearly demonstrated in this exercise.

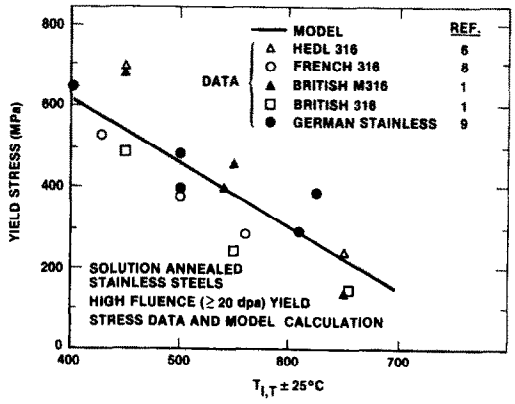

Figure 5. Model Comparisons With Several Other Sets of High Fluence Data for Solution Annealed Stainless Steels.

3. CORRELATION OF DUCTILITY PARAMETERS

Obviously, knowledge of yield stress alone is not sufficient to design engineering structures. Therefore, an attempt was made to correlate changes in an important ductility parameter, uniform elongation, against changes in the yield and ultimate strengths σ_u. Such correlations are of interest for several reasons, including: 1) success or failure of correlations may provide indications of fracture mechanisms; 2) it may be possible to derive only strength data, for example, in an indentation hardness or microtensile test measurements used in small volume high energy neutron experiments (actually, it has been suggested that ductility can be estimated in hardness tests; however, the ductility-strength correlations would provide an independent check on the validity of this assertion).

We have found that uniform elongation ε_u of irradiated and unirradiated stainless steels can be roughly correlated by a simple linear expression

$$\varepsilon_u = C_1 \left(1 - \frac{\sigma_{ys}}{\sigma_u}\right) \qquad (3)$$

where $C_1 \approx .5$ is a function of the macroscopic work hardening coefficient. Figures 6a to c compare predicted uniform elongations as a function of exposure for T = 400 to 600°C using Equation (3), the yield stress model described in Section 2 and an empirical model of $\sigma_u = f(T,dpa)$ derived from the data base. Clearly, the model and experimental results are in agreement only at low temperatures and moderate exposures and at higher temperatures at low exposures. Figure 7 crudely maps the regions where the model is applicable as a function of temperature and exposure; in this case, however, actual σ_{ys} and σ_u data, rather than model calculations, were used to compute ε_u in Equation (3). Closer examination of the data reveals that there is a systematic deviation from Equation (3) which can be approximately expressed in terms of an implicit variation of $C_1 = f(\varepsilon_u,T)$. For example, us-

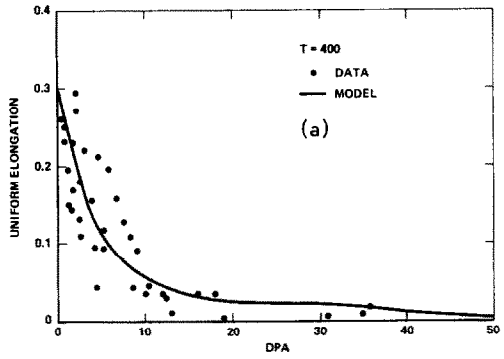

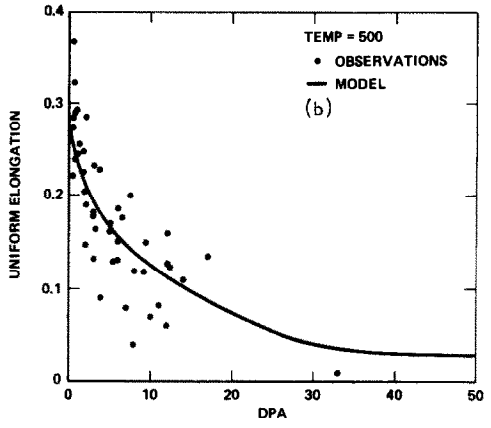

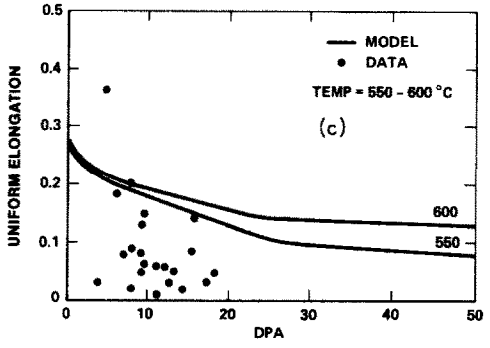

Figure 6. Comparisons of Calculated Ductility Based on Equation 3 With Data at a) 400°C, b) 500°C and c) 550-600°C for Solution Annealed 316 Stainless Steels.

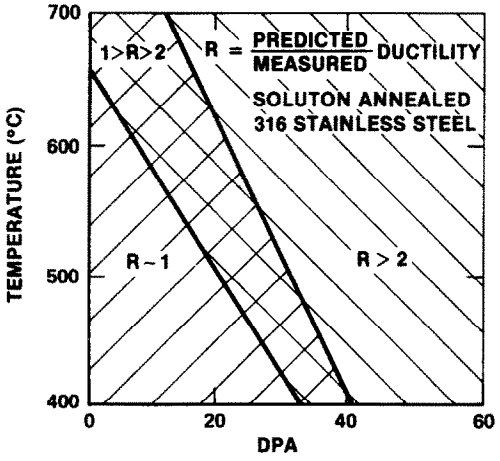

Figure 7. Temperature-Exposure Map of the Ratio of Predicted/Measured Ductility for Solution Annealed 316 Stainless Steel.

ing least squares fits to the data C_1 is .36 for $T > 600°C$ and $\varepsilon_u > 0$, but is only .2 for the range $0 \leq \varepsilon_u \leq .05$; similarly, for $T < 600°C$ C_1 decreases from .52 for $\varepsilon_u > 0$ to .38 for $0 \leq \varepsilon_u \leq .05$.

At high temperatures and moderate to high fluences the deviations may be due to an effect of grain boundary helium, even in relatively high rate tensile tests. Indeed, this is consistent with interpretations given previously [6], which indicate that at increasing temperatures $T \gtrsim 600°C$ a transition between transgranular, flow controlled and intergranular, diffusion or creep controlled fracture occurs; in this regime, a combination of matrix hardening and helium grain boundary embrittlement govern fracture strains. While this interpretation is probably oversimplified, it suggests that the high levels of helium in fusion environments may reduce tensile ductility even more.

The helium mechanism is not, however, a likely explanation of the behavior at lower temperatures and higher fluences, where intragranular ductile fracture is observed. It is of interest, therefore, to consider the microstructure in the various regimes giving rise to the "hardness state" of the alloys. In Section 2 we observed that the major component of the hardening structure is dislocations which develop early in irradiation. If, as suggested in the yield stress calculations, the irradiation induced dislocation structure behaves in a manner roughly equivalent to a similar cold-worked structure, e.g. has similar structure parameters, subsequent deformation should proceed along true stress-strain curve more-or-less normally. At high fluences, however, cavity structures develop and contribute a small but significant fraction to the strength. Hence, subsequent deformations may no longer follow the "normal" dislocation structure dominated path. In particular, severe flow localization, and in the limiting extreme, channel fracture occur under these conditions [2]. Channeling has traditionally been viewed as a consequence of shear induced destruction of dislocation obstacles, such as cavities, and/or reduction in cross slip. Further support to this hypothesis is lent by the fact that 316 has somewhat higher ductility in the cold-worked relative to the solution annealed condition at fluences of 30-40 dpa, since significant void swelling is lower in the cold-worked material [6, 7]. It has been observed that deformation and ductility of cold-worked 316 can be modeled by an unirradiated equation-of-state form up to fluences of 40dpa by making small adjustments of the hardness parameter [10]. This may need to be modified at higher fluences where cavity structures become important.

We will not pursue these speculations further except to note that while the equation-of-state approach is both practically and fundamentally appealing, its use will be greatly enhanced if it can be mechanistically interpreted in terms of specific microstructural features.

4. FRACTURE TOUGHNESS

Clearly, extension of such procedures to other potential fracture properties would be desirable. However, this is not straight-forward since the micromechanical mechanisms are generally significantly more complex and/or there is no appropriate data base for analysis. Further, these properties are generally much more sensitive to test details and conditions. Therefore, we will discuss only briefly some aspects of applying micromechanical models to fracture toughness. We believe, however, that improved creep rupture, crack growth, fatigue and creep-fatigue correlations can also be developed, and this will be pursued in future research.

It is not clear that plane strain fracture toughness K_{Ic} is an appropriate measure of static crack propagation resistance for thin first wall structures (indeed, geometries are likely to be in the plane or, perhaps, even antiplane stress state modes ([11]). However, K_{Ic} should at least provide lower bound effective toughness limits.

A number of micromechanical treatments have been developed to model the effect of tensile properties and microstructure on K_{Ic}. In the simplest form [12]

$$K_{Ic} = \left[\frac{4E}{\pi(1-\nu^2)}\right]^{1/2} (L\,\sigma_y\,\varepsilon_f)^{1/2} \qquad (4)$$

where surface energy terms have been neglected and perfect elastic-plastic behavior assumed. Here E is the Youngs Modulus, ν Poissons ratio, ε_f a fracture strain parameter and L a measure of the effective plastic zone size. Local fracture may be primarily governed by the spacing of ductile fracture cavity nucleation sites or, alternately, propensity towards intensive shear deformation. The choice of a proper ductility parameter (critical strain) is not obvious since it is known to depend on both stress state and work hardening behavior. For convenience, it can be taken as the uniform elongation divided by three to crudely account for stress state. In materials where fracture is dominated by shear instabilities or flow localization, which is likely in the case of irradiated stainless steel, it has been found that $L \alpha n^2$ where n is the work hardening exponent ($\sigma = k\varepsilon^n$); hence Equation (4) becomes

$$K_{Ic} \simeq C_1 n \sqrt{E\,\sigma_y\,\varepsilon_u/3} \qquad (5)$$

and since $n \simeq \varepsilon_u$ and taking $C_1 \sim 1$

$$K_{Ic} \sim \varepsilon_u^{3/2} \sqrt{\sigma_y\ E/3} \qquad (6)$$

Numerous other approaches, including highly sophisticated computer based analyses can be used to attack this problem; however, the current

lack of irradiated stainless steel toughness data suggests that such treatments are not warrented at this time. Figure 8 shows K_{Ic} calculated from Equation (6) using values based on the yield stress model of Section 2 and the empirical ductility correlation procedure of Section 3. Clearly, the model predicts a substantial reduction in toughness of irradiated stainless steels. There is little data to compare with these calculations. The absolute values of the toughness tend to be low by a factor of 1 to 2 compared to some values which have been reported for stainless steel [14 - 16]. Limited data on irradiated (and some shock hardened stainless steel alloys at an approximately equivalent yield strength) in the range of 1 - 10 dpa (equivalent) and temperatures of 250 - 650°C have indicated reductions in toughness of 30 to 50%. This is consistent with the trends indicated in Figure 8. In one case involving both metallurgical differences (weld versus plate) and irradiation, a very large reduction in toughness ∿ 5 was found [17]. The calculations presented here indicate that there may be a significant reduction in toughness in fusion environments. However, data from specifically designed experiments will be needed to determine actual extent and nature of this problem.

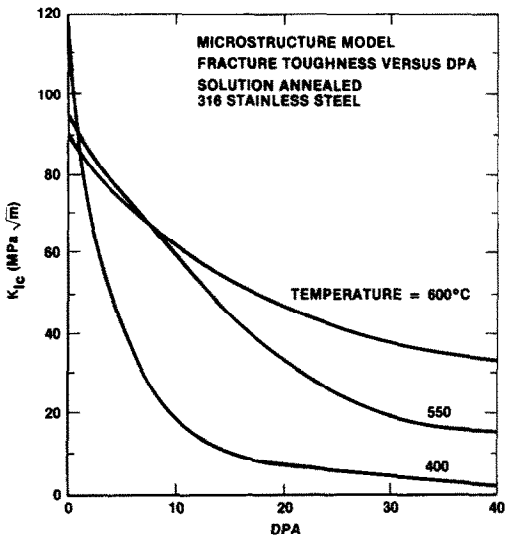

Figure 8. Fracture Toughness Model Calculations.

5. SUMMARY AND CONCLUSIONS

Some initial steps have been taken to develop physically based correlation methods for extrapolating mechanical property data to fusion environments. The yield stress changes in fast reactor irradiations can be correlated with observed changes in microstructure using simple hardening models. Analysis of tensile ductility data suggests that irradiation may change the deformation to fracture path: at higher temperatures this may be associated with grain boundary helium-matrix hardening effects and at lower temperatures with matrix hardening due to shearable cavity structures. A simple micromechanical model was used to extrapolate these calculations to changes in plane strain fracture toughness; while there is not sufficient data to confirm these calculations, the low fluence trends appear to be consistent with limited experimental observations. We conclude, therefore, that microstructural-micromechanical modeling studies will be useful at least when applied to relatively simple properties.

ACKNOWLEDGEMENT

The authors would like to thank Dr. G. Lucas of UCSB and Dr. R. Wullaert of Fracture Control Corporation, Santa Barbara, California, for helpful discussions.

REFERENCES

1. J. Barnaby, D.J. Barton, R.M. Boothly, A.S. Fraser and G.F. Slattery, Radiation Effects in Breeder Reactor Structural Materials, M.L. Bleiberg and J.W. Bennet, Eds. ASM (1977) 159.
2. E.E. Bloom, Radiation Damage in Metals, ASM, (1975) 295.
3. J.J. Holmes and J.L. Straalsund, Ibid. Reference 1, 53.
4. G.R. Odette, Modeling Microstructural Evolution Under Irradiation, this conference.
5. A.L. Bemment, Proceedings of the 2nd Int. Conf. on the Strength of Met. and Alloys 2, ASM (1970) 623.
6. J.J. Holmes, A.J. Lovell and R.L. Fish, Effects of Irradiation on Substructure and Mechanical Properties of Metals and Alloys, ASTM-STP 529 (1974) 383.
7. R.L. Fish and J.D. Watrous, Irradiation Effects on the Microstructure and Properties of Materials, ASTM-STP-611 (1976) 91.
8. J. Dupouy, J. Erler and R. Huillery, Ibid. Reference 1, 83.
9. K. Anderico, L. Shaefer, C. Wassilew, K. Ehrlich and H. Bergman, Ibid. Reference 1, 65.
10. R.W. Fish, N.S. Cannon and G.L. Wire, Tensile Property Correlations for Highly Irradiated 20% C.W. 316 Stainless Steel -- to be published in the Proceedings of the 9th Symp. on Effects of Irrad. on Struc. Alloys, Richland, WA (July, 1978).
11. J.F. Knott, Fundamentals of Fracture Mechanics, John Wiley and Sons, (1973) 116.
12. J.P. Hirth and F.H. Froes, Met. Trans, 8A (1977) 1165.
13. G.T. Hahn and A.R. Rosenfeld, Met. Trans. 6, (1971) 653.
14. F,J. Loss and R.A. Gray, J-Integral Characterization of Irradiated Stainless Steels, NRL Report 7565 (1973).
15. J.W. Sheckherd, M. Kangilaski and A.Braun Instrumented Impact Testing, ASTM-STP-563(1974) 118.
16. J.R. Hawthorne and H.E. Watson, Ibid. Reference 1, 327.
17. J. Dufrense, B. Henry and H. Larsson, Fracture Toughness of Irradiated AISC 304 and 316 Stainless Steels, Ibid. Reference 10.